Raman scattering by intervalley carrier-density fluctuations in *n*-type Si: Intervalley and intravalley mechanisms

G. Contreras,* A. K. Sood,† and M. Cardona
Max-Planck-Institut für Festkörperforschung, Heisenbergstrasse 1, D-7000 Stuttgart 80, Federal Republic of Germany
(Received 22 February 1985)

We present an extensive study of Raman scattering by intervalley density fluctuations in *n*-type Si for a wide range of electron concentrations ($8\times10^{18}\leq N_e\leq10^{20}$ cm^{-3}), temperatures (80—473 K), and laser frequencies (1.16 to 2.54 eV). The experiments were performed with a Raman ($\omega>20$ cm^{-1}) and a Fabry-Perot "Brillouin" spectrometer ($\omega<20$ cm^{-1}). The results indicate that both nonlocal intravalley diffusion and local intervalley scattering contribute to the light scattering. The measured scattering efficiencies can be quantitatively interpreted without recourse to adjustable parameters. Failure to observe the scattering in ion-implanted laser-annealed samples is also discussed.

I. INTRODUCTION

Metals and heavily doped (degenerate) semiconductors can scatter light either through single-particle or collective excitations of free carriers. The single-particle excitations correspond to charge-density fluctuations and, as such, they are screened at low frequencies in a self-consistent manner by the carriers themselves. Thus, in simple, free-electron-like carrier systems no low-frequency scattering is observed. Instead, a peak at the plasma frequency is seen.

In *n*-type silicon the electrons cannot be considered to be such a simple system, as they occupy six equivalent but differently oriented valleys centered along the six equivalent {100} directions. In such multivalley systems, besides the scattering peak at the plasma frequency,[1] scattering by intervalley density fluctuations is seen.[2] Excitations in which the density fluctuations induced in the various equivalent valleys are out of phase and exactly cancel each other become possible. These excitations have no net charge and thus are not collectively screened by the system of carriers. They lead to a low-frequency, Lorentzian-like scattering tail which has been observed in *n*-type Si,[2] *p*-type Si,[3] and, more recently, *n*-type Ge.[4] Attempts to interpret quantitatively the phenomenon with the theory developed by Platzman[5] for free-electron-like systems have failed.[2] The theory proposed by Ipatova *et al.*,[6–8] based on the collision-limited case of electronic transport, seems to be more suitable for the heavily doped semiconductors in which the carriers are strongly scattered by the doping impurities. In this theory the potential corresponding to the incident and scattered fields modulate against each other the energies of the various electron valleys. This modulation encourages intervalley electron transfer through scattering, thus equalizing the Fermi energies of all the valleys. Two types of scattering mechanisms are possible: a local intervalley one, characterized by the scattering time τ_{inter}, in which the required change of crystal momentum is supplied by either phonons or impurities,[6] and a nonlocal one induced by intravalley diffusion from one point of real space to another.[7]

In this paper we present a systematic study of the low-frequency Raman scattering by intervalley density fluctuations in *n*-type Si. Absolute scattering efficiencies are measured in comparison to the scattering by optical phonons in the same samples. The dependence of the scattering efficiency on the scattering frequency is fitted with the theory of Ipatova *et al.*[6–8] The dependence on carrier concentration is shown to follow the predictions of that theory. An investigation of the dependence of the Lorentzian widths of the scattering spectra on scattering wave vectors shows that this width is determined by the intervalley scattering time and also by the intravalley diffusion. From the dependence of the intervalley-scattering time τ_{inter} on temperature and carrier concentration it is shown that τ_{inter} is mainly determined by scattering through LA phonons. The intravalley diffusion constant obtained from the analysis of the Lorentzian widths is compared with predictions from the electron mobility based on Einstein's equation.

II. THEORY

In the collision-limited regime the efficiency for Stokes scattering can be written as[6–8]

$$\frac{\partial^2 S}{\partial\omega\partial\Omega}=(1-e^{-\hbar\omega/k_BT})^{-1}\frac{\omega AB}{\omega^2+A^2}\ , \tag{1}$$

where A is a constant, with the dimensions of frequency, which determines the "Lorentzian" width of the scattering profile. B is a constant with the dimensions of $[(\text{length})\times(\text{frequency})]^{-1}$, k_B is the Boltzmann constant, T the temperature, and Ω the solid angle. Equation (1) represents the efficiency for Stokes scattering per unit length and unit solid angle. The efficiency for anti-Stokes scattering is obtained by replacing ω by $-\omega$ in Eq. (1).

The strength parameter B for *n*-type Si can be written as[6–8]

$$B=\frac{\hbar e^4}{3\pi c^4}\frac{dN_e}{d\eta}\sum_{\alpha=1}^{3}\left|\hat{\mathbf{e}}_L\cdot\left[\frac{1}{\underset{\sim}{m}_\alpha}-\left\langle\frac{1}{\underset{\sim}{m}_\alpha}\right\rangle\right]\cdot\hat{\mathbf{e}}_S\right|^2, \quad (2)$$

where e is the electron charge, c the speed of light, N_e the total electron concentration, η the Fermi energy, $\hat{\mathbf{e}}_L$ ($\hat{\mathbf{e}}_S$) the polarization vectors of the incident (scattered) radiation, $1/\underset{\sim}{m}_\alpha$ the effective-mass tensor, and $\langle 1/\underset{\sim}{m}_\alpha\rangle$ its average over all valleys [$3\langle 1/\underset{\sim}{m}_\alpha\rangle=(2m_\perp^{-1}+m_{||}^{-1})\underset{\sim}{1}$, where for n-type Si $m_\perp=0.19\ m_e$ and $m_{||}=0.98\ m_e$]. The sum in Eq. (2) is performed over the three pairs of valleys $\pm$[100], $\pm$[010], and $\pm$[001]. Equation (2) assumes that all valleys are equally populated. This is true for unstressed n-type Si. If compressive stress along [100] is applied, the $\pm$[100] valleys move down in energy while $\pm$[010] and $\pm$[001] move up. The carriers are all transferred to the *equivalent* $\pm$[100] valleys and the electrons become a one-component system. Thus, the scattering by intervalley density fluctuations disappears. This has been shown to be the case in Ref. 2. The expression for B in the presence of a strain is given in Ref. 6.

In Ref. 6 the intervalley density fluctuations are assumed to be induced only by intervalley scattering. Only the scattering between two valleys at right angles in $\mathbf{k}$ space (e.g., [100] and [010], the so-called f scattering) is effective in producing intervalley fluctuations. That which is between the equivalent [100] and [$\bar{1}$00] valleys (g scattering) does not produce any effect since these valleys are not split by the scattering Hamiltonian. If we call the f-scattering time between two valleys τ_{inter}, we find[6–8]

$$A_0=6\tau_{\text{inter}}^{-1}, \quad (3)$$

where the factor of 6 reflects the existence of *six* valleys.

The intervalley scattering time due to phonons of frequency ω_i can be calculated with the expression[9]

$$\tau_{\text{inter}}^{-1}=\frac{D_i^2 m_d^{3/2}}{(2\pi\rho\hbar\omega_i\hbar^2)^{1/2}}(\eta+\hbar\omega_i)^{1/2}(e^{\hbar\omega_i/k_BT}-1)^{-1}. \quad (4)$$

Equation (4) assumes $k_BT\ll\eta$ and thus includes only phonon absorption processes. D_i is the electron-phonon coupling constant for f scattering, m_d is equal to $(m_{||}m_\perp^2)^{1/3}$, and ρ the density of the crystal. According to Ref. 9, τ_{inter}^{-1} is dominated by scattering by LA phonons ($\omega_i=347\ \text{cm}^{-1}$, $D_i=2.5\times10^8$ eV/cm).

For the purpose of comparison with the experimental data we express τ_{inter}^{-1} in the form

$$6\tau_{\text{inter}}^{-1}=A_{02}(e^{\hbar\omega_i/k_BT}-1)^{-1}. \quad (5)$$

We have listed in Table I the values of A_{02} found with Eqs. (4) and (5) for the samples measured here and also the values found experimentally (see below).

It is also of interest to calculate the intervalley scattering rate due to scattering by the screened ionized impurities. The screening is in this case unimportant since the transfer in wave vector $\kappa=(2\pi/a_0)0.85\sqrt{2}$ (a_0 is the lattice constant) is much larger than the Thomas-Fermi wave vector. Using Fermi's golden rule we find for intervalley scattering

$$\tau_{\text{inter}}^{-1}=\frac{2\pi}{\hbar}\left|\frac{4\pi e^2}{\epsilon(\kappa)\kappa^2}\right|^2 N_e N_d(\eta)$$

$$=\frac{e^4}{\hbar^3}\frac{32\pi^{5/3}m_d}{\epsilon^2(\kappa)\kappa^4 2^{1/3}}N_e^{4/3}\simeq 3.7\left[\frac{N_e}{10^{20}}\right]^{4/3}\text{cm}^{-1}, \quad (6)$$

where N_e should be in cm^{-3} and $\epsilon(\kappa)$ is the dielectric constant of undoped Si for $\omega=0$. Using the expression given in Ref. 10 we find $\epsilon(\kappa)\simeq 2$.

Thus far we have treated the local intervalley scattering. For a density wave with wave vector $\mathbf{q}$ intervalley fluctuations also result from the intravalley diffusion from a minimum to a maximum of the charge density of a given valley. This additional effect can be approximately expressed by replacing A_0 in Eq. (3) by a Lorentzian width A:[7]

$$A=A_0+Dq^2, \quad (7)$$

where $q=4\pi n/\lambda_L$, n being the refractive index and λ_L the laser wavelength, and D is the intravalley diffusion constant which has been assumed to be isotropic (otherwise, it must be replaced by a tensor). This constant is obtained from the electron mobility with Einstein's equation:[11]

$$D=\mu_e\frac{k_BT}{e}\left[\frac{dN_e}{d\eta}\right]^{-1}N_e, \quad (8)$$

where μ_e is the average electron mobility.

TABLE I. Values of A_{01} and A_{02} calculated with Eqs. (4)–(6) (theory) compared with those obtained from the fit of the Raman scattering data (experiment).

Sample[a]	Electron Concentration (cm^{-3})	A_{02} (cm^{-1}) Theory	A_{02} (cm^{-1}) Experiment	A_{01} (cm^{-1}) Theory	A_{01} (cm^{-1}) Experiment
P1	1×10^{20}	154	122	22	49
P2	8×10^{19}	147	118	16	49
As1	5×10^{19}	135	126	8.7	82
P3	2×10^{19}	118	81	2.5	29
P4	8×10^{18}	107	87	0.8	23

[a]P and As stand for phosphorous and arsenic dopants, respectively.

III. EXPERIMENT

Our Raman spectra were taken with a SPEX 1-m double monochromator while the "Brillouin" data were obtained with a five-pass Fabry-Perot spectrometer in the backscattering geometry. Several lines of Ar^+, Kr^+, and Nd yttrium aluminum garnet (YAG) lasers were used, the detection being effected by photon counting.

The samples were x rays oriented to within 1°. The scattering surface was polished to optical flatness with Syton (Monsanto Chemical Co.) and then treated with HF. The carrier concentrations (Table I) were determined from the minimum in the ir reflectivity and the resistivity.[12,13] For low-temperature measurements the samples were glued with silver paint to the cold finger of a liquid-nitrogen cryostat, the temperature measured by a thermocouple attached to the sample. For high-temperature measurements the sample was placed inside a small resistive oven surrounded by an evacuated quartz envelope to prevent oxidation.

IV. RESULTS AND DISCUSSION

Typical low-frequency scattering spectra taken at 80 K for the samples listed in Table I are shown in Fig. 1.

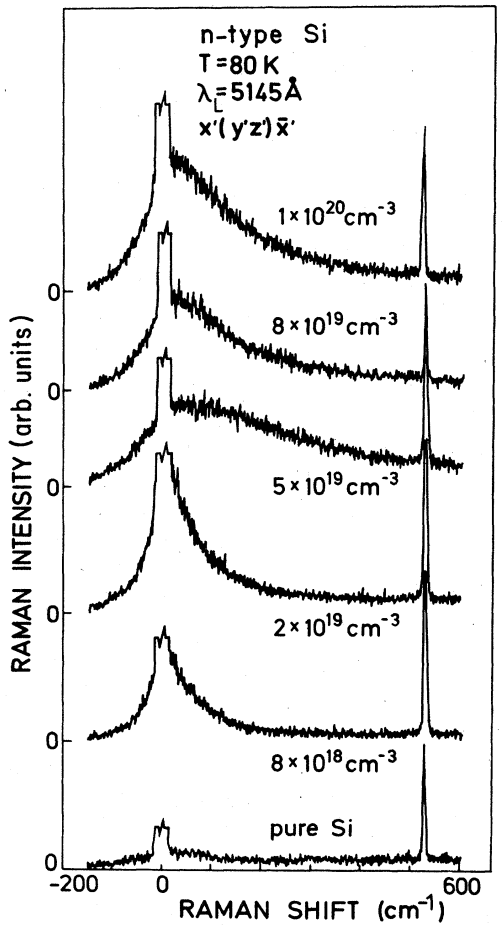

FIG. 1. Typical electronic Raman spectra at 80 K for the five samples listed in Table I. The sharp line on the Stokes side is the Raman phonon, forbidden in the scattering configuration used. It nevertheless appears weakly, perhaps due to polarization leakage and slight misorientation of the sample.

These spectra were obtained with the 5145-Å line of the Ar^+ laser in the Γ_{12} scattering configuration $[\mathbf{x}'(\mathbf{y}'\mathbf{z}')\bar{\mathbf{x}}'$, where $\mathbf{x}'$, $\mathbf{y}'$, $\mathbf{z}'$ are along the (001), (110), and (1$\bar{1}$0) crystal axes, respectively. $\mathbf{x}'$ and $\bar{\mathbf{x}}'$ indicate the direction of the incident and scattered beam, $\mathbf{y}'$ and $\mathbf{z}'$ that of $\hat{\mathbf{e}}_L$ and $\hat{\mathbf{e}}_S$, respectively]. According to Eq. (2) the Raman tensor for scattering by intervalley density fluctuations is expected to have the symmetry of the tensor,

$$\frac{1}{m_\alpha}-\left\langle\frac{1}{m_\alpha}\right\rangle,$$

i.e., for n-type Si, with the valleys along {100} and Γ_{12} symmetry (E in molecular notation). The pure Γ_{12} depolarized configuration $\mathbf{x}'(\mathbf{y}'\mathbf{z}')\bar{\mathbf{x}}'$ was chosen to avoid the second-order structure due to two TA phonons, which appears strongly in the Γ_1 configuration,[14] i.e., in any polarized configuration, and also to maximize stray light rejection. We also performed measurements in the $\Gamma_{25'}$ configuration $\mathbf{x}'(\mathbf{y}'+\mathbf{z}',\mathbf{y}'-\mathbf{z}')\bar{\mathbf{x}}'$, in which no low-frequency scattering is seen, thus confirming the Γ_{12} nature of the corresponding Raman tensor. In the $\Gamma_{25'}$ configuration we observed the Raman phonon of silicon. Since its absolute scattering efficiency is known,[15,16] we used it to calibrate the efficiency of the Γ_{12} scattering by intervalley density fluctuations. In this manner, the scattering spectrum (in absolute efficiency units of $\partial^2 S/\partial\Omega\partial\omega$) shown in Fig. 2 for $N_e=10^{20}$ cm^{-3}, was obtained. Note that the point (represented by an asterisk) obtained at 10 cm^{-1} with a Brillouin spectrometer (calibrated with respect to the acoustic phonons[15,16]) agrees reasonably well with the results of the Raman spectrometer; the scattering intensities are seldom measured to better than 30%.

The Raman data of Fig. 2 were fitted with Eq. (1). The results of this fit are shown by the solid line in this figure. The fit is excellent. The values of B obtained from the fit are plotted in Fig. 3 versus N_e. They should be proportional to $dN_e/d\eta$, the density of states at the Fermi energy, which, in the case $k_BT \ll \eta$, is proportional to $N_e^{1/3}$. We have thus fitted the experimental results with a curve proportional to

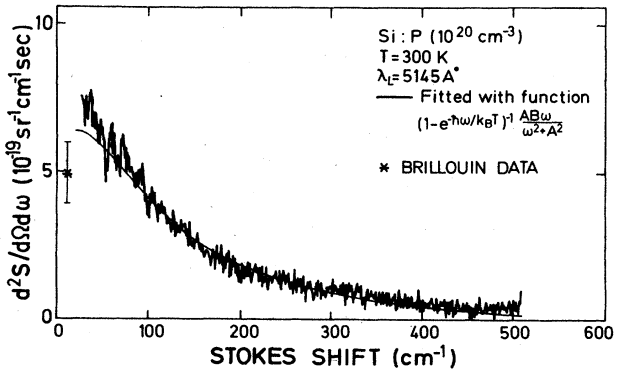

FIG. 2. Electronic Raman line shape (efficiency in absolute units) for the heaviest doped sample at 300 K. The solid line represents the curve of Eq. (1), obtained with A and B as adjustable parameters. The point (*) was obtained at 10 cm^{-1} with a Fabry-Perot spectrometer.

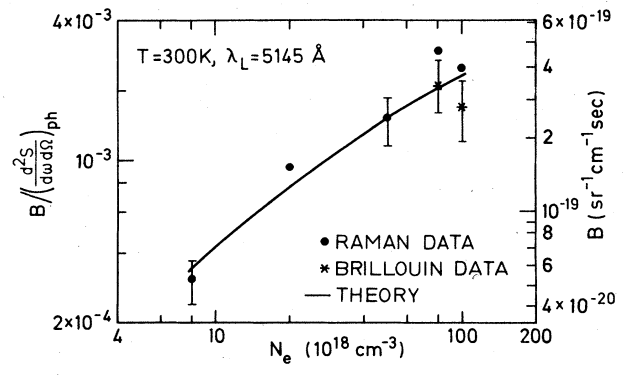

FIG. 3. Parameter B normalized to the height of the scattering by Raman phonons in the $\mathbf{x}'(\mathbf{y}'\mathbf{z}')\bar{\mathbf{x}}'$ configuration. The solid line represents a fit with Eq. (2). The absolute values of B (right-hand scale) were obtained with the value of $dS/d\Omega = 1.25\times10^{-4}$ sr^{-1}cm^{-1} found in Ref. 16 at 5145 Å and the phonon line with a half width at half maximum of 1.3 cm^{-1} from Ref. 20.

$$\frac{dN_e}{d\eta} = \frac{N_c}{2k_BT} F_{-1/2}\left[\frac{\eta}{k_BT}\right], \quad N_c = 12(2\pi m_d k_B T\hbar^{-2})^{3/2} . \tag{9}$$

The results of the fit, which is quite satisfactory, are displayed by the solid line in Fig. 3. The coefficient of the fit in Fig. 3 should be compared with the results of the calculation with Eq. (2): We find the theoretical B to be eight times lower than the experimental one. This discrepancy can be reduced if one considers the fact that Eq. (2) is only valid for $\omega_L, \omega_S \ll \omega_g$, where ω_g is the gap which determines the effective masses in $\mathbf{k}\cdot\mathbf{p}$ theory.[15] This gap E_g amounts to about 4 eV in n-type Si (slightly less than the E_2 gap or the gap at the X point[17]), which is only less than twice as large as the photon energy used in Fig. 3 (2.41 eV). Thus, if we neglect the longitudinal inverse mass $m_{\|} \gg m_{\perp}$, in Eq. (2) we should multiply the prediction of Eq. (2) by the enhancement factor[15]

$$\left[\frac{E_g}{2}\left[\frac{1}{E_g-\hbar\omega_L}+\frac{1}{E_g+\hbar\omega_S}\right]\right]^2 , \tag{10}$$

which for $\hbar\omega_L = 2.41$ eV amounts to $\simeq 2.5$. Hence, the discrepancy between the theory of Eq. (2) and the experimental results is partly removed when the resonance enhancement factor of Eq. (10) is taken into account. A discrepancy by a factor of 3 remains, the experiment being larger than the theory. A discrepancy in the same direction, but somewhat larger, has also been found in n-type Ge.[4] This discrepancy is not too serious when one considers that typical measurements of absolute cross sections in solids are affected by errors of about 50%. One may, however, speculate that the explanation for the discrepancy lies in the way the resonance enhancement has been introduced in the phenomenological, collision-limited theory. Thus, a microscopic treatment, dealing with the intervalley and intravalley scattering in perturbation theory on the same microscopic level as the resonance, is needed.

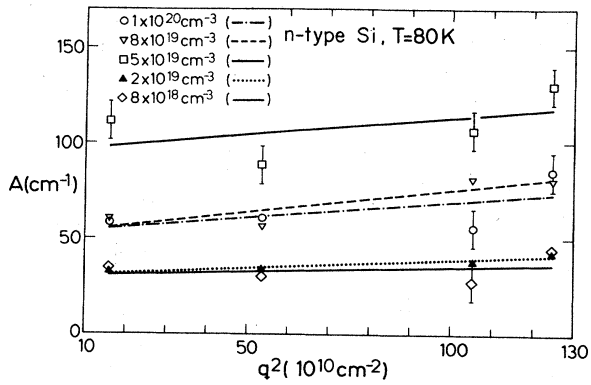

FIG. 4. Dependence of A on the square of the scattered wave vector. Solid and dashed lines are fitted according to Eq. (7).

We show in Fig. 4 the dependence of A on q^2 found experimentally (points) and the corresponding least-squares fit with Eq. (7). Despite the large error bars involved, it appears clear that the experimental A's include both intervalley scattering ($A_0 \neq 0$) and intravalley diffusion ($D \neq 0$) contributions. We note that the data for the one As-doped sample measured fall out of line with those for P-doped samples of almost the same carrier concentration ($A_0 \sim$ two times higher). The larger A_0 is difficult to understand: it is difficult to believe that As ions produce a larger intervalley scattering than that given simply by the Coulomb potential of Eq. (6) [the pseudopotential of As is actually *closer* to that of Si than that of P (Ref. 10)]. There may, however, be As clusters or other defects which may produce large f-type intervalley scattering. A systematic investigation of As-doped samples is required before reaching any definite conclusions.

The dependence of A on N_e for the P-doped samples is shown in Fig. 5 for different laser wavelengths (i.e., q's) at 80 K. The lines in this figure were calculated with Eqs. (6) and (7) using the value of A_0 obtained from Fig. 4 and the values of μ_e given in Ref. 18. For our purpose the

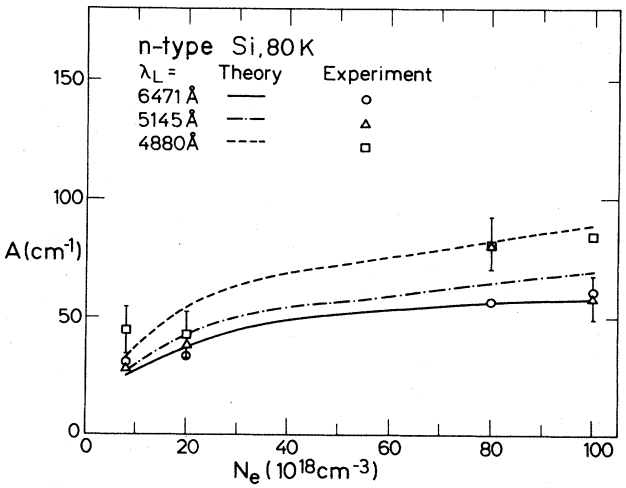

FIG. 5. Electron concentration dependence of A. The solid and dashed lines represent calculations based on Eqs. (7) and (8).

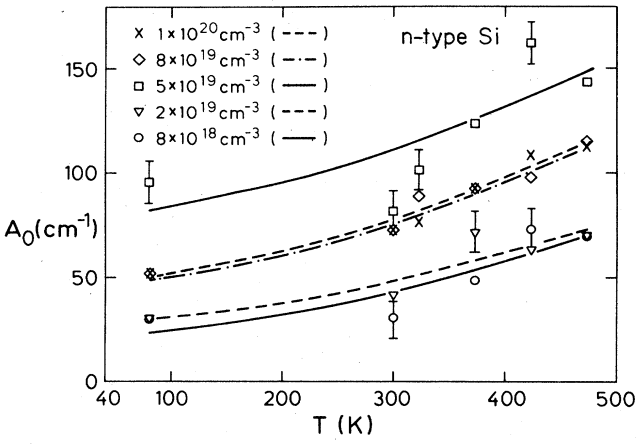

FIG. 6. Temperature dependence of A_0. The solid and dashed lines represent fittings done according to Eq. (11).

mobility μ_e of the heavily doped samples can be assumed to be independent of temperature.

The intercepts of the plots of Fig. 4, and similar ones for other temperatures, yield the values of A_0 which have been plotted as points in Fig. 6 versus temperature. The lines in this figure represent fits to the experimental points with the equation

$$A_0 = A_{01} + A_{02}(e^{\hbar\omega_i/k_BT} - 1)^{-1}, \tag{11}$$

where A_{01} represents the contribution of the impurities to the intervalley scattering [of Eq. (6)] and A_{02} that of the phonons [of Eq. (5)]. A_{01} and A_{02} were used here as fitting parameters. The values of A_{01} and A_{02} so obtained for the various samples measured are listed in Table I. The agreement between theoretical and calculated values of A_{02} is quite good. For A_{01} the agreement is good at the highest doping levels but the experimental A_{01} decreases with decreasing N_e more slowly than the theoretical $N_e^{4/3}$ [Eq. (6)]. Part of the discrepancy surely lies in the assumption of degenerate statistics, made in the derivation of Eq. (6), which should not hold for the less-doped samples. We feel, however, that our data are not sufficiently accurate to warrant a fit taking into account the temperature dependence of A_{01} relative to the statistics of the free electrons.

Several unsuccessful attempts were made to observe light scattering by intervalley density fluctuations in samples produced by ion implantation and laser annealing,[19] with carrier densities up to 10^{21} cm^{-3}. The most likely reason for the absence of observable effects in these samples is the possible existence of a very large A_{01} due to defects in these samples. This large A_{01} would broaden the Lorentzian of Eq. (1) to the point of making it unobservable (below the noise level).

V. CONCLUSIONS

We have presented a detailed study of the light scattering due to carrier-density fluctuations in n-type Si as a function of the carrier concentration, temperature, and scattering wave vector. Our results demonstrate the contribution of both intervalley (local) and intravalley (nonlocal) relaxation mechanisms to these Raman spectra, the former being usually dominant. Although the theory of Refs. 6 and 7 explains the results well, a discrepancy still remains between the calculated and experimental values of the quantity B. This discrepancy is brought down to a factor of 3 when resonance enhancement of the "effective mass" is taken into account. A microscopic theory taking into account the intervalley and intravalley relaxations on the same level as the resonance enhancement of the effective masses is needed.

ACKNOWLEDGMENTS

We would like to thank I. P. Ipatova and her Leningrad co-workers for a number of enlightening discussions about their work. Thanks are also due to H. Hirt, P. Wurster, and M. Siemers for their skillful technical help. We also thank J. Wagner for his help in recording the spectra with the Nd-YAG laser. G. C. acknowledges financial support from the Deutscher Akademischer Austauschdient.

*Permanent address: Escuela Superior de Física y Matemáticas—Instituto Politécnico Nacional, Edificio 6, Unidad Profesional Adolfo López Mateos, Delegacion G.A. Madero, 07300 México, Distrito Federal, México.

†Permanent address: Materials Science Laboratory, Reactor Research Centre, Kalpakkam-603102, India.

[1]N. Mestres, F. Cerdeira, and M. Cardona, in *Proceedings of the 17th International Conference on the Physics of Semiconductors, San Francisco, 1984,* edited by J. Chadi and W. E. Harrison (Springer, New York, 1985).

[2]M. Chandrasekhar, M. Cardona, and E. O. Kane, Phys. Rev. B **16**, 3579 (1977).

[3]M. Chandrasekhar, U. Rössler, and M. Cardona, Phys. Rev. B **22**, 761 (1980).

[4]G. Contreras, A. K. Sood, and M. Cardona, following paper, Phys. Rev. B **32**, 930 (1985).

[5]P. M. Platzman, Phys. Rev. **139**, A379 (1965).

[6]I. P. Ipatova, A. V. Subashiev, and V. A. Voitenko, Solid State Commun. **37**, 893 (1981).

[7]I. P. Ipatova, A. V. Subashiev, and V. A. Voitenko, J. Raman Spectros. **10**, 221 (1981).

[8]G. Abstreiter, M. Cardona, and A. Pinczuk, in *Light Scattering in Solids IV,* Vol. 54 of *Topics in Applied Physics,* edited by M. Cardona and G. Güntherodt (Springer, Heidelberg, 1984), p. 5.

[9]C. Jacoboni, R. Minder, and G. Majni, J. Phys. Chem. Solids **36**, 1129 (1975).

[10]L. Viña and M. Cardona, Phys. Rev. B **29**, 6739 (1984).

[11]N. G. Nilsson, Phys. Status Solidi **19**, K75 (1973).

[12]P. A. Schumann, Jr., Solid State Technol. **13**, 50 (1970).

[13]V. I. Fistul, *Heavily Doped Semiconductors* (Plenum, New York, 1969).
[14]P. A. Temple and C. E. Hathaway, Phys. Rev. B **7**, 3685 (1973).
[15]M. Cardona, in *Light Scattering in Solids II,* Vol. 50 of *Topics in Applied Physics,* edited by M. Cardona and G. Güntherodt (Springer, Heidelberg, 1982), p. 19.
[16]M. H. Grimsditch and M. Cardona, Phys. Status Solidi B **102**, 155 (1980).
[17]J. Chelikowski and M. L. Cohen, Phys. Rev. B **14**, 556 (1976).
[18]C. Yamanouchi, K. Mizuguchi, and W. J. Sasaki, Phys. Soc. Jpn. **22**, 859 (1967).
[19]A. Compaan, G. Contreras, M. Cardona, and A. Axmann, J. Phys. (Paris) Colloq. **44**, C5-197 (1983).
[20]J. Menéndez and M. Cardona, Phys. Rev. B **29**, 2051 (1984).